Analysis & Suppression of Low-Frequency Noise (LFN) in Dielectric-Modulated-Trench Junctionless Indium Arsenide Antimonide (InAsSb) Dual-Gate (DG) FET-Biosensors by Variation of Arsenic Mole-Fraction

PALASRI DHAR[1], SWAGATA BHATTACHERJEE[2], SUNIPA ROY[3*], TANVIR HABIB SARDAR[4*], MAHENDRA KUMAR GOURISARIA[5], AHAMED SHAFEEQ B M[6]

[1] Guru Nanak Institute of Technology, Kolkata 700114, India (purba.dhar@gmail.com)
[2] Techno India, Saltlake, Kolkata-700091(swagata.bhattacherjee@gmail.com)
[3] Guru Nanak Institute of Technology, Kolkata 700114, India(sunipa_4@yahoo.co.in)
[4] Department of CSE, Dayananda Sagar University, Bangalore, 562112, India (tanvir.sardar@gmail.com)
[5]Department of CSE, School of Computer Engineering, KIIT Deemed to be University, Bhubaneswar - 751024, Odisha, India, (mkgourisaria2010@gmail.com)
[6] Department of CSE, Manipal Institute of Technology, Manipal Academy of Higher Education, Manipal, India 576104, (ahamed.shafeeq@manipal.edu)

Corresponding authors: sunipa_4@yahoo.co.in, tanvir.sardar@gmail.com

ABSTRACT

This paper reveals the low-frequency noise of an Indium Arsenide Antimonide (InAsSb) channel dielectric modulated trench gate junctionless Dual-Gate FET (DG FET) and demonstrates that low-frequency noise in a DG FET can be suppressed by changing the mole fraction of arsenic in the Indium Arsenide Antimonide (InAsSb) channel dielectric modulated trench gate junctionless Dual-Gate FET. The effects of the Arsenic composition on the Junctionless InAsSb DG FET device's sensitivity and performance against low-frequency noise are investigated. The results ensure that composition fraction plays a very important role in the Streptavidin, APTES and Ferro-cytochrome biomolecules detection and reduction of the low-frequency noise. According to the current investigation, a significant quantity of low-frequency noise can be produced by either a low or high content of Arsenic. For neutral and charged biomolecules at 1 Hz frequency, an intermediate molar percentage of Arsenic, ideally between 45% and 65%, can efficiently suppress the noise and produce a signal-to-noise ratio of greater than 10^4 in the Dielectric-Modulated Trench Junctionless Indium Arsenide Antimonide (InAsSb) Dual-Gate(DG) FET.

Keywords: Biosensor, dielectric modulated, JL FET, drain current, sensitivity, trench-gate.

INTRODUCTION

Biotechnology fosters various sustainable approaches for the upswing of agricultural areas through pre-investigation of the state of land and water resources and the use of chemicals like pesticides and fertilisers to increase production. It also identifies with the culinary and healthcare sectors and has many uses. Extreme outbreaks of novel diseases brought on by unknown biohazards have made early detection of biomolecules and their comprehensive and precise analysis vital. As dielectric-modulated field effect transistors (FETs) provide a high degree of label-free sensing by nature, they have become more appealing for biomolecule spotting [1-5]. One of the most critical parameters for biosensors is sensitivity, which is influenced by both the kinds of biomolecules and the device architectures. Charged biomolecules can alter the cavity's interface-trapped charge densities and dielectric constants.

The trapped charges at the interface between the conducting channel and the dielectric layer directly cause low-frequency noise, which significantly reduces the device's sensitivity, particularly for charged biomolecules. Numerous FET-based biosensors with various device topologies, such as tunnel FETs [6-12], impact ionization FETs (IMOS) [13], and junctionless FETs [14-19], were proposed in various studies. A few studies also addressed III-V channel material-based sensors [20–22]. Nevertheless, there are not many publications that discuss biosensor noise analysis. [23] focuses on the RTS noise for the single trap phenomenon and shows noise suppression for nano transistor biosensors beyond the temperature limit. In [24], a small signal model for noise is introduced for Bio FET devices, where flicker noise is thought to be the main noise source, with thermal noise from the electrolyte resistance contributing slightly. In [25], LFN is also investigated for single-gate extended sources. For silicon nanowire sensors, the effects of device settings on power spectral density were examined in [26]. In [27], the subthreshold region, the signal-to-noise ratio for charge sensing, is optimized for liquid-gated SWNT transistors. investigated the noise source in biosensors based on carbon nanotubes [28]. They found that interaction between substrates and adsorbates increases charge noise. The effects of high-k dielectrics and cavity thickness on junctionless DG FETs are thoroughly examined in [29].

However, silicon is used as the channel material in the aforementioned reports. Noise negatively influences device performance and works better with no silicon materials, such as silicon oxide, where high-k dielectric layers are used instead. In biosensors, noise enters electrochemical interfaces when charges are transferred [30]. LFN's huge time constants for bio-detection make it more effective than other noise sources. The first thing we address in this research is the noise analysis of an InAsSb channel trench gate JL DG FET for neutral and charged biomolecules. We identify the optimal performance of the device by thoroughly examining the effects of the Arsenic(As) molecule's molar fraction on the biosensor's low-frequency noise parameters and performance indicator

DEVICE STRUCTURE & SIMULATION FRAMEWORK

As shown in Figure 1, a trench gate JL DG FET is taken into consideration in the current work. The two vertical gates are placed in separate trenches on either side of the channel. When biomolecules are not present, two vertical nanogaps that are filled with air form between the channel and gates.

Accordingly, the gate and drain connections are applied. When biomolecules are not present, it is assumed to be filled with air and the value of di-electric constant is considered as 1, which is adjusted based on the dielectric constant of the biomolecules. This change in the dielectric constant causes a variation in the gate capacitance, which is reflected in the device's transconductance and drain current, among other electrical properties. We use SILVACO ATLAS simulator to simulate the device as well as to study its characteristics. Fermi-Dirac statistics, concentration-dependent mobility and field-dependent carrier mobility, velocity saturation, and band gap narrowing models are employed for the simulation. We extract different parameters of the channel materials, such as band gap, electron affinity, permittivity and intrinsic carrier concentrations for different Arsenic (As) compositions for employment in simulation [31]. Various electrical parameters, like surface potential, drain current, transconductance, etc., are obtained from the simulation. Relevant device parameters are listed in Table 1.

Modelling of low-frequency noise

If a change of gate bias δV_g causes a change in drain current (δI) and drain current may be considered as the combination of unwanted fluctuation (I_{UF}) and useful signal (I_{US}) then

$$\partial I = \partial I_{US} + \partial I_{FL} \qquad (1)$$

where δIus and δIFL are the change in useful current and unwanted fluctuation respectively, then SNR is defined as [16]

$$SNR = \frac{\partial I_{US}}{\partial I_{FL}} \qquad (2)$$

For FET-based biosensors, threshold voltage shift (δV_{th}), because of the interaction of biomolecules can be considered a signal [16], and the SNR can be defined as:

$$SNR = \frac{\partial V_{th}}{\sqrt{\int_{f_1}^{f_2} S_{VG}}} \quad (3)$$

where S_{VG} is the equivalent input-referred voltage noise and is obtained as [17]

$$S_{VG} = \frac{q^2 kT\lambda N_t}{f^v wL_g C_{eff}^2}\left[1+\frac{\alpha\mu_{eff} c_{eff} I_D}{g_M}\right] \quad (4)$$

Here, details of all the parameters are given in [32].

The normalised drain current power spectral density is obtained as [18]:

$$\frac{S_{ID}}{I_D^2} = S_{VG} \times \left(\frac{g_M}{I_D}\right)^2 \quad (5)$$

Using ATLAS I_D, g_M, V_{SG} and δV_{th} are obtained, and using Eq. (4) & Eq. (5), the other noise parameters are calculated.

SILVACO ATLAS simulates the electronic noise by calculating the statistical behaviors of equivalent random voltage sources at its ports. A small volume of the device is to get the noise from the entire part of the device. The impact ionization and the Hooge model are applied to enable LFN. SNR is a crucial parameter for biosensors as it determines the degree of detection by the signal level for noise. Tracing bio-species also depends on the presence of intrinsic noise in the device. The impact ionization and the Hooge model are applied to enable LFN. SNR is a crucial parameter for biosensors as it determines the degree of detection by the level of signal concerning noise. Tracing bio-species also depends on the presence of intrinsic noise in the device.

MODELLING OF PERMITTIVITY OF InAsSb:

If the $InAs_xSb_{1-x}$ material energy band gap is computed as:

$$E_{gInAs_xSb_{1-x}} = xE_{gInAs} + (1-x)E_{gInSb} - x(1-x)C_{Eg} \quad (6)$$

here,

E_{gInAs} is the bandgap of binary InAs computation with x= 1,

$E_{gInAs_xSb_{1-x}}$ is the band-gap of InAsxSb(1-x),

E_{gInSb} is the bandgap of binary InAs computation with x= 0.

C_{Eg} is the bowing factor Band gap,

It is calculated that the $InAs_xSb_{1-x}$ material's electron affinity is:

$$\chi InAs_{1-x}Sb_{1-x} = x\chi_{InAs} + (1-x)\chi_{InSb} - x(1-x)C_\chi \quad (7)$$

here,

$\chi InAs_{1-x}Sb_{1-x}$ is the electron affinity of $InAs_xSb_{1-x}$

χ_{InAs} is the electron affinity of InAs.

χ_{InSb} is the electron affinity of InSb.

The value of the bowing factor of electron affinity (C_x) is calculated as :

$$C_\chi = C_{E_g}\frac{dE_c}{dE_g} \quad (8)$$

$\frac{dE_c}{dE_g}$ is the parameter of alignment. The value is taken as 0.5.

The conduction band density of states effective mass longitudinal and transverse directions electrons of $InAs_xSb_{(1-x)}$ is computed as:

$$m*_{C_{InAs_xInSb_{1-x}}} = \left(m*^{2}_{ct_{InAsSb}} \times m*_{cl_{InAsSb}}\right)^{\frac{1}{3}} \quad (9)$$

Here, $m*_{cl_{InAsSb}}$ and $m*_{ct_{InAsSb}}$ are conduction band Density of states effective mass in longitudinal and transverse directions in $InAs_xSb_{(1-x)}$.

In Eq. (9) the values are taken as :

$$m*_{cl_{InAsSb}} = xm*_{cl_{InAs}} + (1-x)m*_{cl_{InSb}} \quad (10)$$

and

$$m*_{ct_{InAsSb}} = xm*_{ct_{InAs}} + (1-x)m*_{ct_{InSb}} \quad (11)$$

The valence band density of state effective mass of $InAs_xSb_{(1-x)}$ for heavy and light holes is computed as :

$$m*_{h_{InAs_xInSb_{1-x}}} = \left(m*^{\frac{3}{2}}_{lh_{InAs_xInSb_{1-x}}} + m*^{\frac{3}{2}}_{hh_{InAs_xInSb_{1-x}}}\right)^{\frac{2}{3}} \quad (12)$$

In Eq. (12) the values are taken as:

$$m*_{hh_{InAsSb}} = xm*_{hh_{InSb}} + (1-x)m*_{hh_{InAs}} \quad (13)$$

and

$$m*_{lh_{InAsSb}} = xm*_{lh_{InAs}} + (1-x)m*_{lh_{InSb}} \quad (14)$$

The permittivity(ε) of $InAs_xSb_{(1-x)}$ is calculated as:

$$\varepsilon_{InAs_xSb_{1-x}} = \chi_{\varepsilon_{InAs}} + (1-\chi)\varepsilon_{InSb} \quad (15)$$

MODEL CALIBRATION

The simulation model is calibrated against the reported experimental data[33]. Figure 2 shows the simulated transfer characteristics of the dielectric modulated trench gate DG $InAs_xSb_{1-x}$ channel JLFET for a gate length of 50 nm at 50 mV and 0.5 V drain voltages, which is compared with reported experimental data [33].

The combined trench and dual-gate structure enhance electrostatic control, reduces short-channel effects, and ensures accurate prediction of LFN behavior. The trench gate geometry confines the electric field laterally, minimizing leakage and enabling sensitive dielectric modulation by biomolecules, while the dual-gate configuration improves gate-to-channel coupling, directly influencing the transconductance term (g_M) as in Eq. (4) and Eq. (5).

In the SILVACO ATLAS simulations, several calibrated physical models such as, Fermi–Dirac carrier statistics, field- and concentration-dependent mobility, velocity saturation, and bandgap narrowing, were applied to accurately represent carrier transport in the InAsSb alloy. The Hooge noise model and impact ionization model was included to capture flicker noise and LFN sources. The calibration shown in Figure 2, confirms strong agreement between simulated and experimental data [33], validating the precision of the simulation approach. Hence, the chosen architecture and model set enable realistic LFN predictions and reliable sensitivity evaluation of the proposed biosensor.

RESULT & DISCUSSIONS

A. Study of Dielectric-Modulated Trench Junctionless InAsSb DG--FET sensitivity and biosensing attributes:

We have studied the Dielectric-Modulated Trench Junctionless InAsSb DG--FET sensitivity in terms of Drain current and transconductance efficiency (g_M/I_D), which are of the important performance indicators [34] in effective detection of the biomolecules .

Figure 3 represents the transfer characteristics of the biosensor in the presence and absence of bio species having dielectric constants 1, 2.1, 3.57 and 4.7. These are the dielectric constant of Streptavidin, APTES and Ferro-cytochrome respectively.

The graph indicates the detection of the biomolecules of Streptavidin, APTES and Ferro-cytochrome by showing a large difference in the drain current with biomolecules such as k=2.1,k=3.57 and k=4.7 w.r.t the air (k=1) in the subthreshold region.

Figure 4 depicts the Transconductance efficiency (g_M/I_D) change with drain current for different dielectric constant k , such as, k=2.1,k=3.57 and k=4.7 w.r.t the air (k=1). The presence of biomolecules changes the transconductance efficiency from 12 (k=1) to 16, 22 and 24 when k values are 2.1, 3.57 and 4.7. This change is due to different biomolecules such as Streptavidin, APTES and Ferro-cytochrome in the cavity space. So, this Dielectric-Modulated Trench Junctionless InAsSb DG-FET can effectively detect biomolecules and can be called a biosensor.

B. Noise analysis for neutral biomolecules:

As indicated in Figure 4, g_M/I_D changes sharply w.r.t air in the presence of biomolecules, which ensures the sensing capability of bio species. This change of g_M/I_D increases the k value of bio species.

In Figure 5, the variation of g_M/I_D with gate voltage for different values of composition fraction ,i.e, x is presented. It is noteworthy that g_M/I_D, which is equivalent to the device's gain, is influenced a lot by x. It means the detection capacity can be improved by the proper selection of x.

Figure 6. demonstrates the frequency response of input-referred noise (S_{VG}) and normalized drain current power spectral density (S_{ID}/I_D^2) for different bio species such as Streptavidin, APTES and Ferro-cytochrome. The figure indicates that the bio species with a higher k value generates more noise. Thus, noise suppression is also significant in detecting different biomolecules.

The frequency response of Input referred Noise(S_{VG}) is depicted in Figure. 7 and Figure. 8 for different values of x, and it is found that S_{VG} is reduced by increasing x, but the exact nature is revealed in Figure 8, where both the S_{VG} and S_{ID}/I_D^2 are plotted against x for different bio-samples. The intermediate As mole fraction ($x \approx 0.45–0.65$) provides an optimal balance between carrier concentration and trap density.

In Figure 9, the graph shows that noise factors are reduced by increasing the composition fraction , x, reaching its optimum value, and increasing with x, although the trend is against the spotting of biomolecules. We explore the SNR for different biomolecules, which is an important biosensor parameter that needs to be investigated.

The variation of SNR is shown and it is observed that SNR can be improved by choosing the mole fraction ~ 65% of As. As shown in Figures 7–9, S_{VG} and S_{ID}/I_D^2 and both exhibit minima in this As composition range, while the SNR that is defined by Eq. (2) exceeds 10^4 at 1 Hz frequency. Therefore, the intermediate arsenic fraction optimizes electronic transport and trap suppression, resulting in both lower LFN and higher biosensor sensitivity.

The variation in the arsenic (As) mole fraction within the InAsSb channel directly governs the low-frequency noise (LFN) characteristics and overall sensitivity of the dielectric-modulated trench junctionless dual-gate (DG) FET biosensor. Adjusting the As composition modifies key material properties such as bandgap, electron affinity, and carrier mobility, thereby influencing both the charge transport and noise generation mechanisms in the channel. At lower As compositions, the narrower bandgap results in a higher intrinsic carrier concentration and stronger carrier fluctuations, leading to increased flicker noise (*1/f*) and degraded signal stability. At higher As contents, the increased bandgap and reduced mobility enhance scattering and trap-assisted noise, again elevating the total LFN.

The intermediate As mole fraction ($x \approx 0.45–0.65$) provides an optimal balance between carrier concentration and trap density. This composition minimizes both the input-referred voltage noise (S_{VG}) and normalized drain current power spectral density S_{ID}/I_D^2 as defined in Eq. (4) and Eq.(5) of the manuscript. These relations quantify the voltage and current noise behavior derived from the SILVACO ATLAS simulations, linking the microscopic carrier fluctuations to macroscopic noise performance. Simulation results (Figures 7–9) demonstrate that in this composition range, the LFN is significantly suppressed, while the signal-to-noise ratio (SNR) exceeds 10^4 at 1 Hz. Hence, tuning the arsenic mole fraction in the InAsSb channel effectively controls the noise–mobility trade-off, ensuring both high sensitivity and low noise operation in the trench junctionless DG FET biosensor.

C. Noise analysis for charged biomolecules:

Noise factors are strongly influenced by the trapped charges associated with the bio-samples, and the impacts are not the same for positive and negative charges. Thus, noise factors may differ for neutral and charged biomolecules. In this paper, we consider both the donor and acceptor type trapped charges and set the distance of the donor trap level from the conduction band (E. level) as 0.46 eV.

We consider the trapping cross-section 10^{-15} cm^2 and vary the charge density from 5×10^{10} cm^{-2} to 1×10^{12} cm^{-2}. Fig. 10 presents the I-V characteristics for positive and negatively charged biomolecules for a fixed dielectric constant, whereas Figure 11 shows the g_M/I_D vs gate voltage. It is observed that the drain current reduces when the charge density changes towards its negative value (N_d^+ to N_d^-), especially in the subthreshold and weak inversion region, g_M/I_D decreases with decreasing N_d^+ and increasing N_d^- in the subthreshold region, but the peak value of g_M/I_D does not depend on the charge density or its nature; it only depends on the gate voltage.

We studied the noise factors for different mole fractions, as represented in Figure 12 – Figure 14. In Figure. 12, a variation of SVG is observed with the charge density of biomolecules for different x, whereas in Figure 12, the same observables are studied for different bio species. From both figures, it is confirmed that S_{VG} decreases with decreasing N_d^- and increasing N_d^+. This means that the LFN is more significant for negatively charged bio species. Figure 14 depicts the SNR for charged biomolecules, where it is found that SNR improves for +ve charged biomolecules. For all three cases, betterment of noise parameters is observed for a 65 % molar fraction of the as atom.

Different biomolecules influence the biosensor's noise behavior through their dielectric properties and surface charge densities. Neutral biomolecules (such as Streptavidin and APTES) modulate the gate capacitance without introducing net charge, thereby affecting transconductance and threshold voltage shifts that determine sensitivity (as expressed in Eq. (3) for SNR). In contrast, charged biomolecules introduce additional electrostatic interactions and interface-trap occupancy, significantly impacting the noise spectral density(S_{ID}/I_D^2)and input-referred voltage noise SVG) defined in Eqs. (4) and Eq. (5).

Simulation results in Figures 10–14 show that negatively charged biomolecules increase LFN due to enhanced trap-assisted tunnelling, while positively charged biomolecules reduce LFN and improve SNR. Despite these variations, the biosensor maintains robust performance, with $S_{ID}/I_D^2<10{-}7$ when the arsenic mole fraction is optimized near 0.65. These findings confirm that the device retains high sensitivity and low noise operation across a range of biomolecule charge states.

CONCLUSION

The comparison of I_{Dbio}/I_{Dair} and sensitivity for $InAs_XSb_{1-X}$ channel biosensor with other reported works are shown in Table 2 and as seen from the table the values of SNR, S_{ID}/I_D^2 and S_{VG} are much more improved as compared to the other reported works. We have presented the analysis of LFN for the presence of neutral and charged biomolecules for an InAsSb channel dielectric modulated trench gate junctionless DG FET. Results indicate that the sensitivity of biomolecules can be improved by decreasing the mole fraction of as at the expense of LFN. The input-referred voltage noise, the normalized drain current power spectral density, and SNR improve by increasing the mole fraction in the range of 60 – 65 per cent of as for neutral and charged biomolecules. In the case of charged bio species, noise level depends on the polarity of charge. Negatively charged biomolecules generate more noise than positive ones. Thus, special care should be taken in spotting negative bio species.

ACKNOWLEDGMENT

We gratefully acknowledge DST, Govt of India (FIST-level 0, Sanction letter no: SR/FST/COLLEGE-466/2018) for providing laboratory and equipment support.

REFERENCES

[1] Rawat, Brajesh & Paily, Roy. "Analysis of Graphene Tunnel Field-Effect Transistors for Analog/RF Applications.," Electron Devices, IEEE Transactions on. 62. 2663-2669. https://doi.org/10.1109/TED.2015.2441092 (2025).
[2] Svintsov, Dmitry & Vyurkov, V. & Lukichev, et al. "Tunnel field-effect transistors with graphene channels" Semiconductors.47. https://doi.org/10.1134/S1063782613020218 (2013)
[3] Ramedani, A., Sabzevari, O., Simchi, A. "Processing of liposome-encapsulated natural herbs derived from Silybum marianum plants for the treatment of breast cancer cells." Scientia Iranica ; 29(6): 3619-3627. https://doi.org/10.24200/sci.2022.61070.71309 (2022).
[4] Faramarzi, V., Ahmadi, V., Ghane Golmohamadi et. al. "A biosensor based on plasmonic wave excitation with diffractive grating structure." Scientia Iranica; 24(6): 3441-3447. https://doi.org/10.24200/sci.2017.4253 (2017).
[5] Debata, P. P., Mohapatra, P. "A Modified Metaheuristic Algorithm Integrated ELM model for Cancer Classification." Scientia Iranica,; 29(2): 613-631. https://doi.org/10.24200/sci.2022.56265.4630 (2022)
[6] S. Kanungo, S. Chattopadhyay, P. S. Gupta et. al. "Comparative Performance Analysis of the Dielectrically Modulated Full- Gate and Short-Gate Tunnel FET-Based Biosensors," in IEEE Transactions on Electron Devices, vol. 62, no. 3, pp. 994-1001. https://doi.org/10.1109/TED.2015.2390774 (2015)
[7] Dwivedi, Praveen and Abhinav Kranti. "Applicability of Transconductance-to-Current Ratio as a Sensing Metric for Tunnel FET Biosensors." IEEE Sensors Journal: 1030-1036, https://doi.org/10.1109/JSEN.2016.2640192 (2017).
[8] P. Dwivedi and A. Kranti, "Dielectric Modulated Biosensor Architecture: Tunneling or Accumulation Based Transistor," in *IEEE Sensors Journal*, vol. 18, no. 8, pp. 3228-3235, https://doi.org/10.1109/JSEN.2018.2808948 (2018)
[9] Verma, Madhulika et al. "Performance Assessment of a Novel Vertical Dielectrically Modulated TFET-Based Biosensor." *IEEE Transactions on Electron Devices* 64: 3841-3848, https://doi.org/10.1109/TED.2017.2732820 (2017)
[10] Arjmandi,N.,Seraj,M. "Fabrication of a solution-processed IGZO/NiO p-n diode."Scientia Iranica; 31(21): 1963-1970,https://doi.org/10.24200/sci.2023.57301.5166 (2024)
[11] Naz, R., Sohail, M., Bibi, M., et. al."Numerical treatment of magneto hydrodynamic Carreau liquid with heat and mass transport containing gyrotactic microorganisms." Scientia Iranica; 30(6): 2223-2234, https://doi.org/10.24200/sci.2021.54398.3731 (2023).
[12] Beiki, Z., Jahanian, A. "RTL2DNA: An automatic flow of large-scale DNA-based logic circuit design." Scientia Iranica, 2023; 30(4): 1279-1295, https://doi.org/10.24200/sci.2022.54993.4017 (2023).
[13] Kumar, Mamidala Jagadesh, N. Kannan et. al. "Dielectric-Modulated Impact-Ionization MOS (DIMOS) Transistor as a Label-free Biosensor", IEEE Electron Device Letters, Vol.34. https://doi.org/10.1109/LED.2013.2283858 (2013).
[14] Mohammad K. Anvarifard, "Symmetrical SOI MESFET with a dual cavity region (DCR-SOI MESFET) to promote high-voltage and radio-frequency performances" Superlattices and Microstructures, Volume 98,Pages 492-503,ISSN 0749-6036, https://doi.org/10.1016/j.spmi.2016.09.003 (2016).
[15] Behniafar, M., Mahjur, A., Nowroozi, A. "Anomaly Detection Fog (ADF): A federated approach for internet of things." Scientia Iranica,; 30(2): 465-476. https://doi.org/10.24200/sci.2022.57774.5410 (2023).
[16] Topaloglu, I. "Deep Learning Based Convolutional Neural Network Structured New Image Classification Approach for Eye Disease Identification."Scientia Iranica, ; 30(5): 1731-1742. https://doi.org/10.24200/sci.2022.58049.5537 (2023).
[17] Sattar Akbari Nakhjavani, Hadi Mirzajani, Sandro Carrara, Mehmet C. Onbaşlı.Advances in biosensor technologies for infectious diseases detection.TrAC Trends in Analytical Chemistry, 180,117979,0165-9936, https://doi.org/10.1016/j.trac.2024.117979 (2024).
[18] Wadhwa, G., Raj, B. "Label Free Detection of Biomolecules Using Charge-Plasma-Based Gate Underlap Dielectric Modulated Junctionless TFET ". *J. Electron. Mater.* **47**, 4683–4693. https://doi.org/10.1007/s11664-018-6343-1 (2018).
[19] Dwivedi, Praveen & Kranti, Abhinav "Applicability of Transconductance-to-Current Ratio (gm/Ids) as a Sensing Metric for Tunnel FET Biosensors." IEEE Sensors Journal. PP. 1-1, https://doi.org/10.1109/JSEN.2016.2640192 (2016).
[20] Narang, Rakhi et al. "A Dielectric-Modulated Tunnel-FET-Based Biosensor for Label-Free Detection: Analytical Modeling Study and Sensitivity Analysis." *IEEE Transactions on Electron Devices* 59 : 2809-2817, , https://doi.org/10.1109/TED.2012.2208115 (2012).
[21] Dawit Burusie Abdi, M. Jagadesh Kumar, "Dielectric modulated overlapping gate-on-drain tunnel-FET as a label-free biosensor" Superlattices and Microstructures, Volume 86,Pages 198-202,ISSN:0749-6036, https://doi.org/10.1016/j.spmi.2015.07.052 (2015).
[22] Ajay Kumar, M.M. Tripathi, Rishu Chaujar, "Sub-30nm In2O5Sn gate electrode recessed channel MOSFET: A biosensor for early-stage diagnostics", Vacuum, Volume 164,Pages 46-52,ISSN 0042-207X, https://doi.org/10.1016/j.vacuum.2019.02.054 (2019).
[23] S. Kumar, B. Singh and Y. Singh, "Analytical Model of Dielectric Modulated Trench Double Gate Junctionless FET for Biosensing Applications," in *IEEE Sensors Journal*, vol. 21, no. 7, pp. 8896-8902, https://doi.org/10.1109/JSEN.2021.3056385 (2021).
[24] S. Kumar, Y. Singh, B. Singh and P. K. Tiwari, "Simulation Study of Dielectric Modulated Dual Channel Trench Gate TFET-Based Biosensor," in *IEEE Sensors Journal*, vol. 20, no. 21, pp. 12565-12573, https://doi.org/10.1109/JSEN.2020.3001300 (2020).

[25] A. Bhattacharyya, M. Chanda and D. De, "Analysis of Noise-Immune Doping-less Heterojunction Bio-TFET Considering Partial Hybridization Issue," in IEEE Transactions on Nanotechnology, vol. 19, pp. 769-777, https://doi.org/10.1109/TNANO.2020.3033966 (2020)

[26] Kutovyi, Y., Madrid, I., Zadorozhnyi, I. et al. "Noise suppression beyond the thermal limit with nano-transistor biosensors". Sci Rep **10**, 12678. https://doi.org/10.1038/s41598-020-69493-y (2020).

[27] M. J. Deen, M. W. Shinwari, J. C. Ranuárez, D. Landheer; Noise considerations in field-effect biosensors. J.Appl.Phys.; 100(7): 074703. https://doi.org/10.1063/1.2355542 (2006).

[28] Talukdar, J., Rawat, G., Singh, K. et al. "Low Frequency Noise Analysis of Single Gate Extended Source Tunnel FET." Silicon **13**, 3971–3980. https://doi.org/10.1007/s12633-020-00712-x (2021).

[29] Kristine Bedner et al.,Investigation of the dominant 1/f noise source in silicon nanowire sensors, Sensors and Actuators B: Chemical,Volume191,Pages 270-275,ISSN 0925-4005, https://doi.org/10.1016/j.snb.2013.09.112 (2014).

[30] Shiu-Ming Huang, Wei-Chueh Cheng, Pin-Cing Wang, Fu-En Cheng, Chiu-Hsien Wu. Significant Enhancement of NO2 Detection Response in MoTe2 Nanostructures with a 1T′-2H Structure Mixture. *ACS Applied Nano Materials*, *7* (1) , 306-312. https://doi.org/10.1021/acsanm.3c04506 (2024).

[31] Tal Sharf, Joshua W. Kevek, Tristan DeBorde, et. al. "Origins of Charge Noise in Carbon Nanotube Field-Effect Transistor Biosensors", Nano Letters 12 (12), 6380-6384, https://doi.org/10.1021/nl303651t (2012).

[32] S.Bhattacherjee, P.Dhar, S.Roy "Impacts of Cavity Thickness and Insulating Material on Dielectric Modulated Trench Junction-less Double Gate Field Effect Transistor for Biosensing Applications", Current Materials Science; Volume 17, Issue 5, Year 2024, e201023222455, https://doi.org/10.2174/0126661454274311231011070702 (2024).

[33] Anvarifard, Mohammad. "Modeling a Double-Halo-Doping Carbon Nanotube FET in DC and AC Operations." ECS Journal of Solid State Science and Technology. 7. M209-M216. https://doi.org/10.1149/2.0191812jss (2018).

[34] Bhattacherjee, S., Biswas, A. "Investigation on noise performance of $InAs_xSb_{1-x}$ MOSFETs with compositional variations." *Microsyst Technol* **26**, 1133–1140. https://doi.org/10.1007/s00542-019-04639-1 (2020).

[35] C. Convertino *et al*., "InGaAs-on-Insulator FinFETs with Reduced Off-Current and Record Performance," *IEEE International Electron Devices Meeting (IEDM)*, San Francisco, CA, USA, pp. 39.2.1-39.2.4, https://doi.org/10.1109/IEDM.2018.8614640 (2018).

[36] Pavithra S, Ashis Tripathy, Girija Shankar Sahoo, Dusan Losic. "Junction less tunnel field-effect transistors (JLTFET): A transformation from design to diagnosis."Materials Science in Semiconductor Processing, Volume 192,2025,109402:1369-8001, https://doi.org/10.1016/j.mssp.2025.109402 (2025).

[37] Kumari Nibha Priyadarshani, Sangeeta Singh, Mustafa K.A. Mohammed. "Dielectric/charge density modulated junctionless FET based label-free biosensor," Inorganic Chemistry Communications, Volume 148,110350:1387-7003,https://doi.org/10.1016/j.inoche.2022.110350 (2023).

[38] Bousari, N.B., Anvarifard, M.K. & Haji-Nasiri, S. "Benefitting from High-κ Spacer Engineering in Balistic Triple-Gate Junctionless FinFET- a Full Quantum Study". *Silicon* **12**, 2221–2228 . https://doi.org/10.1007/s12633-019-00318-y (2020).

[39] Pavithra S, Ashis Tripathy, Girija Shankar Sahoo, et. al. "Junction less tunnel field-effect transistors (JLTFET): A transformation from design to diagnosis" Materials Science in Semiconductor Processing, Volume 192,109402,ISSN 1369-8001, https://doi.org/10.1016/j.mssp.2025.109402 (2025).

List of Figure Captions:

FIGURE 1. Schematic diagram of InAsSb channel trench gate DG JL dielectric modulated biosensor

FIGURE 2. Calibration of the present device with the result obtained from [33].

FIGURE 3. Transfer characteristics for different bio species.

FIGURE 4. Variation of gM/ID with ID for different biomolecules for As mole fraction=0.25.

FIGURE 5. Change of gM/ID with VGS for different x at k=3.57.

FIGURE 6. Plot of Input referred noise and normalized drain current power spectral density as a function of f for different bio species.

FIGURE 7. Frequency response of SVG for different values of x.

FIGURE 8. Variation of SVG and SID/ID2 with x for different bio species.

FIGURE 9. Impact of x on SNR for different biomolecules.

FIGURE 10.Variation of ID with VG for different charged species.

FIGURE 11.Plot of gM/ID with VGS for different charged species.

FIGURE 12.Impact of charge density on SVG for different x.

FIGURE 13.Variation of SVG with charged species for different k values.

FIGURE 14.Dependence of SNR on charged bio species

List of table captions:

TABLE 1: DIFFERENT PARAMETERS OF DIELECTRIC-MODULATED TRENCH JUNCTIONLESS INDIUM ARSENIDE ANTIMONIDE DUAL GATE FET

Table 2. COMPARISON OF I_{Dbio}/I_{Dair} and SENSITIVITY FOR $InAs_XSb_{1-X}$ CHANNEL BIOSENSOR with other reports

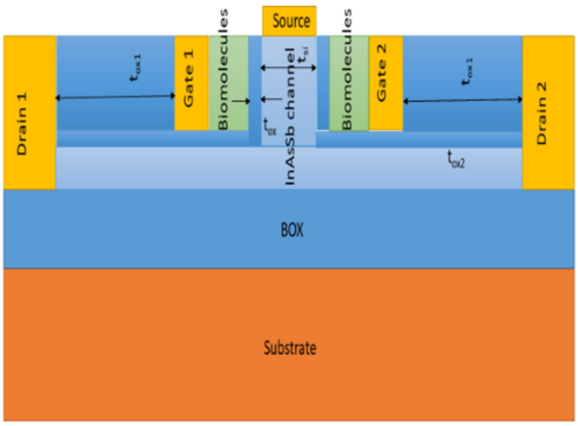

Figure 1, Schematic diagram of InAsSb channel trench gate DG JL dielectric modulated biosensor

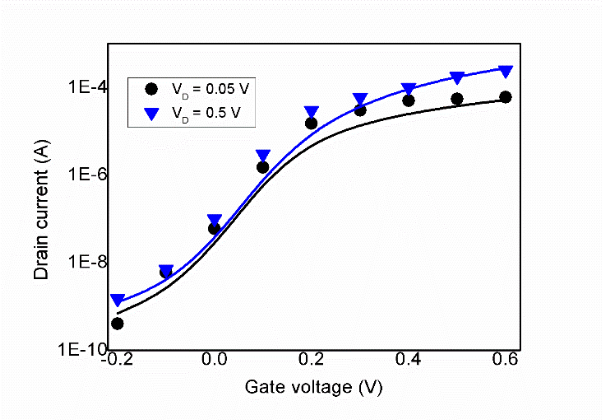

FIGURE 2. Calibration of the present device with the result obtained from [33].

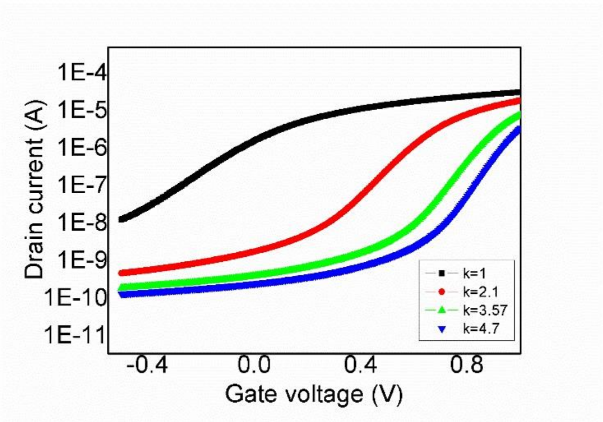

Figure 3 .Transfer characteristics for different bio species

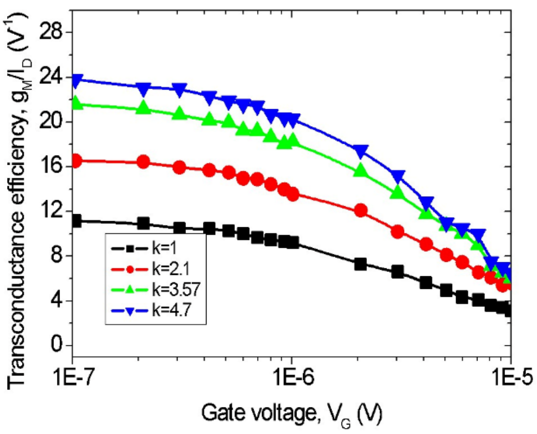

FIGURE 4. Variation of g_M/I_D with ID for different biomolecules for As mole fraction=0.25

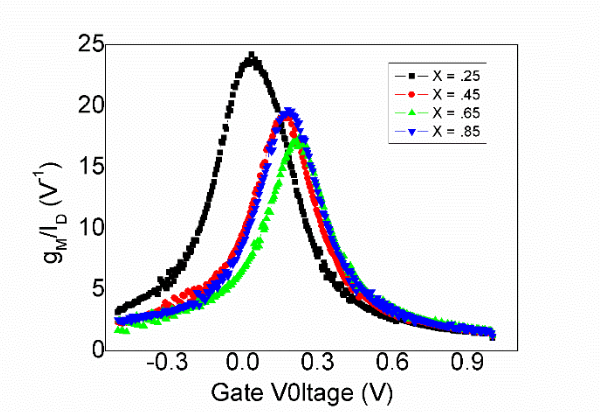

FIGURE 5. Change of g_M/I_D with VGS for different x at k=3.57.

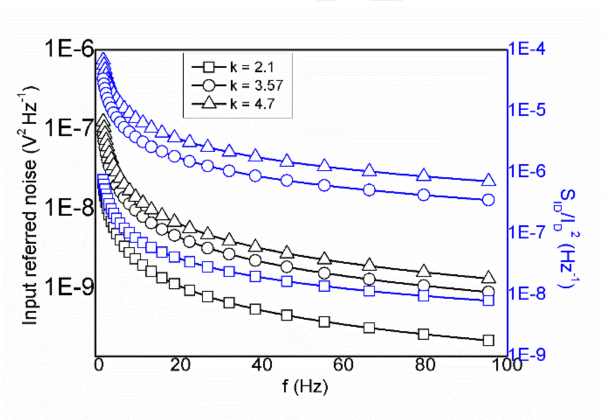

FIGURE 6. Plot of Input referred noise and normalized drain current power spectral density as a function of f for different bio species

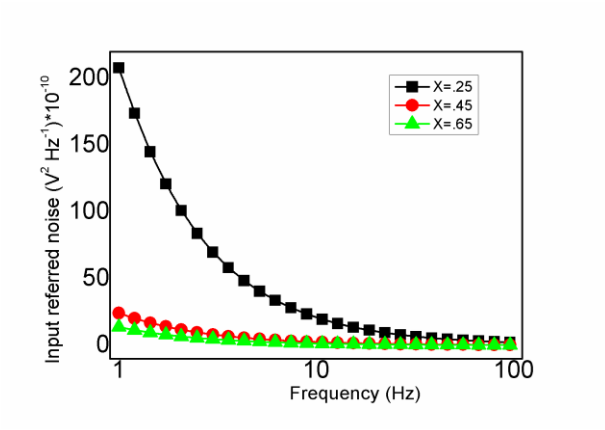

FIGURE 7. Frequency response of S_{VG} for different values of x

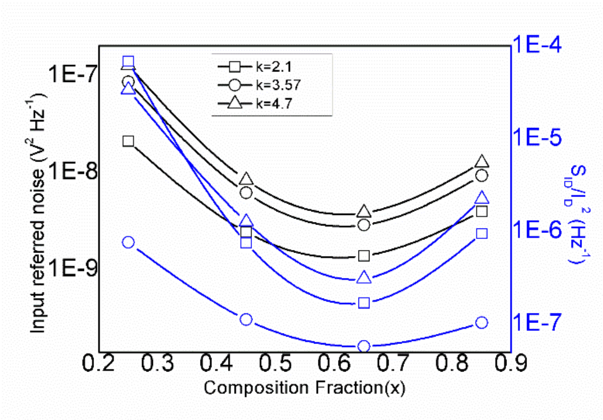

FIGURE 8. Variation of SVG and S_{ID}/I_D^2 with x for different bio species

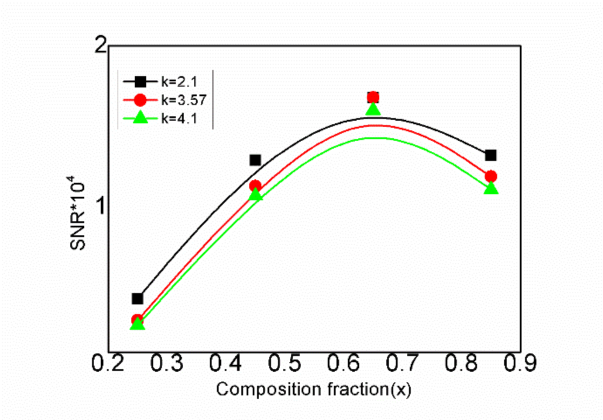

FIGURE 9.Variation of SVG and S_{ID}/I_D^2 with x for different bio species

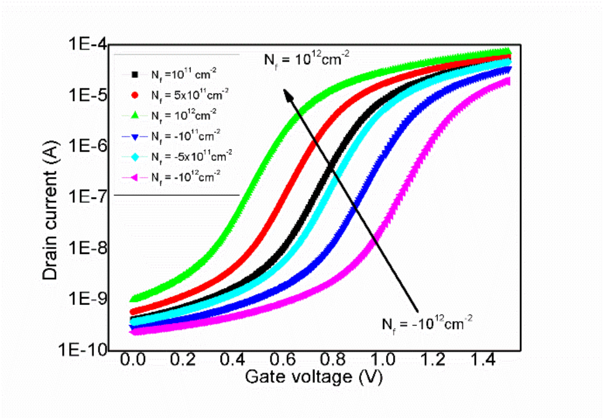

FIGURE 10. Variation of I_D with V_G for different charged species.

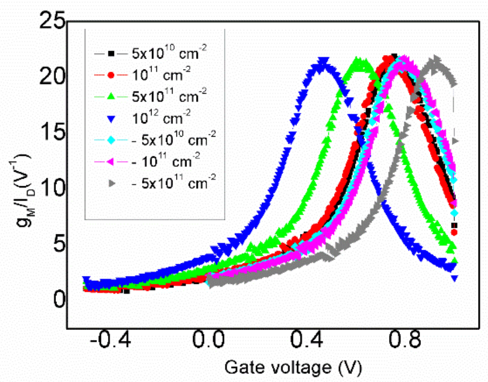

FIGURE 11. Plot of g_M/I_D with V_{GS} for different charged species.

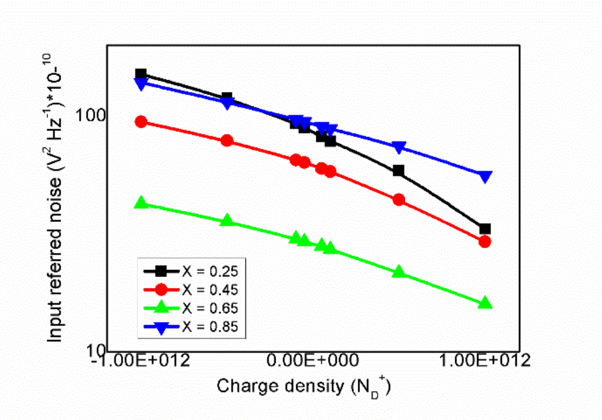

FIGURE 12. Impact of charge density on S_{VG} for different x

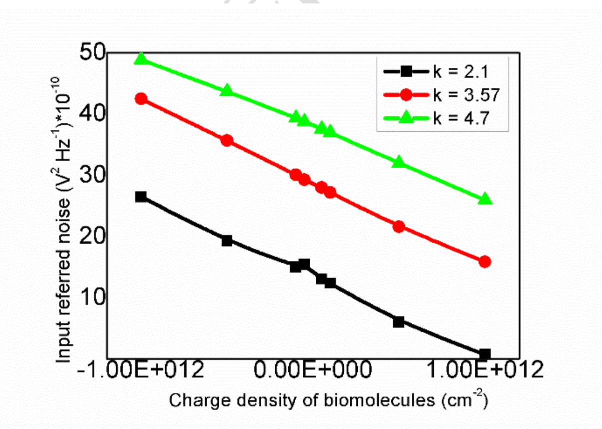

50
40
30
20
10
Input referred noise (V^2 Hz^-1)*10^-10
-1.00E+012
0.00E+000
1.00E+012
Charge density of biomolecules (cm^-2)
k = 2.1
k = 3.57
k = 4.7

FIGURE 13. Variation of S_{VG} with charged species for different k values

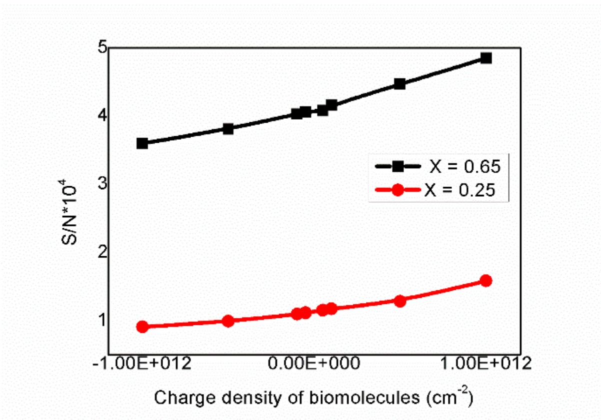

FIGURE 14. Dependence of SNR on charged bio species

TABLE 1: DIFFERENT PARAMETERS OF DIELECTRIC-MODULATED TRENCH JUNCTIONLESS INDIUM ARSENIDE ANTIMONIDE DUAL GATE FET

Parameters	**Value**
Gate length	50 nm
Channel doping concentration	1×10^{18} cm-3
Drain doping concentration	1×10^{19} cm-3
Gate oxide thickness	1 nm
Thickness of nanogap	5
Length of nanogap	50 nm
Drain bias	0.5 V
Gate bias	-0.5 V-1.6 V
The dielectric constant of biomolecules	2.1,3.57 & 4.7
Charge density of biomolecules	-1×10^{12} cm-2 - 1×10^{12} cm-2
Molar fraction of As	0.25-0.85

Table 2. COMPARISON OF I_{Dbio}/I_{Dair} and SENSITIVITY FOR $InAs_XSb_{1-X}$ CHANNEL BIOSENSOR with other reports

Device specification	Frequency (Hz)	SNR (Max)	S_{ID}/I_D^2 (Hz^{-1}) (Min)	S_{VG} (V^2Hz^{-1}) (Min)	Ref
CNT transistor [20]	1	6×10^3	-	-	[20]
Si Nanowire Transistor [19]	10	-	1.2×10^{-10}	1.2×10^{-10}	[19]
N-type NW FETs	10	1.2×10^2	-	2×10^{-8}	[23,35-39]
Present work (neutral biomolecules)	1	1.68×10^4	5.75×10^{-8}	1.37×10^{-9}	

Biographies:

Palasri Dhar received the M.Tech. degree in VLSI and microelectronics from West Bengal University of Technology, Kolkata, India, in 2012. She is currently pursuing the Ph.D. degree at the Department of Electronics and Telecommunication Engineering, Maulana Abul Kalam Azad University of Technology, West Bengal. Her current research interests include Nanomaterials, Biosensors, and modelling of nano devices. She is currently working as Assistant Professor of Electronics and Communication engineering Guru Nanak Institute of Technology, Kolkata, India.

Dr. Swagata Bhattacherjee obtained her M.Sc. in Electronic Science from University of Calcutta in 2004. She awarded her Ph.D from Radio Physics and Electronics in 2012 on nanoscale device modeling. Her area of interest is modeling of MOSFET, TFET, JLFET and Biosensor. She is working as Asst. Professor in Dept. Of Physics,Techno India Saltlake.

Dr Sunipa Roy received her PhD degree from Jadavpur University, Electronics and Telecommunication Engineering department. She is presently serving as Dean, Research and Development at Guru Nanak Institute of Technology, Kolkata, India. Her current research interest includes Nanomaterials, Graphene and Gas Sensors.She has more than 100 publications in high impact factor journal & conferences. She authored many books for international publishers. Dr. Roy is the senior member of IEEE, regular reviewer of IEEE journals and published several patents. Presently she is acting as a Secretary, IEEE CASS Kolkata Section and IEEE Student Branch Counsellor of Guru Nanak Institute of Technology. She is supervising several PhD theses.

Tanvir Habib Sardar is currently an Associate Professor in the Department of Computer Science and Engineering at Dayanand Sagar University, Bangalore. He received his M.Tech degree in Computer Science and Engineering from Visvesvaraya Technological University, Karnataka, India, in 2014. He earned his PhD degree in the area of Big Data and Distributed Computing in 2022 from Visvesvaraya Technological University, Karnataka, India. He has published more than 60 research articles, 17 patents and has published 10 books.

Mahendra Kumar Gourisaria received his bachelor’s degree in commerce with (Hons) from Calcutta University, master’s degree in computer application from Indira Gandhi National Open University, New Delhi, and M.Tech degree in computer science and engineering (CSE) from Biju Patnaik University of Technology, Rourkela. He completed his PhD degree in CSE from Kalinga Institute of Industrial Technology, Deemed to be University, Bhubaneswar, Odisha. He has completed ICWAI (intermediate) from the Institute of Cost and Works Accountants of India and DNIIT from NIIT Sahid Nagar, Bhubaneswar. Currently, he is working as Associate Professor [I] in the School of Computer Engineering, KIIT Deemed to be University. He has an experience of more than 22 years in academia and ten years in research. He has published more than 240 research papers in different book chapters, international journals, and conferences of repute. His Google Scholar citation is more than 2700 with an H-index of 26 and an i10-index of 64. He has received the Research Achievement Award from (IUILA 2024) London Metropolitan University. His research interests include cloud computing, machine learning, deep learning, data mining, soft computing, and internet and web technology. He is a member of IAENG and UACEE; and a Life Member of ISTE, CSI, and ISCA. He has served as an organizing committee member for various conferences and workshops, chaired sessions in many international conferences, and a reviewer for many reputed journals, such as Springer and Hindawi, and many reputed conferences.